Appl. Phys. A (2017) 123:129
DOI 10.1007/s00339-017-0755-2

Applied Physics A
Materials Science & Processing

Thermal annealing studies of the deep level emission in solution-grown zinc oxide nanorods

Crispin Munyelele Mbulanga[1] · Z. N. Urgessa[1] · S. R. Tankio Djiokap[1] · J. R. Botha[1]

Received: 29 October 2016 / Accepted: 1 January 2017
© Springer-Verlag Berlin Heidelberg 2017

Abstract In this report, the effects of thermal annealing on the room temperature (RT) photoluminescence characteristics of solution-grown ZnO nanorods (ZNs) are presented. It is shown that the near surface regions of as-grown ZNs are rich in Zn. Within the detection limit of X-ray photoelectron spectroscopy (XPS), it is confirmed that the environment of annealing affects indeed the activation of intrinsic defects. Furthermore, thermal treatment at high temperatures removes H-related defects as expected; and this removal process is found to affect significantly the RT luminescence properties of ZNs, especially when ZNs are annealed sequentially from 300 °C to ~700 °C. Specifically, the passivation of vacancy-related defects by H is demonstrated following thermal treatment in this temperature range. Finally, the green luminescence (~500 nm) that evolves following annealing above ~800 °C is assigned to Zn vacancy defects.

1 Introduction

Zinc oxide (ZnO) is a semiconductor with interesting properties, such as a large direct band gap and a stable free exciton, even above room temperature. Its high band gap (~3.37 eV) ensures a large breakdown field, and the thermal stability of the material allows high temperature operation. These properties make ZnO an ideal compound for high power and high temperature electronic devices, and have sparked substantial effort among researchers [1–5]. A growing interest exists in quasi-one-dimensional ZnO, such as nanorods, nanowires, nanobelts and nanotubes. They are considered as potential candidates for applications, such as gas sensors [6], biosensors [1, 2], nanolasers [3], optical waveguides [5], and light emitting diodes [3]. It is widely believed that ZnO nanostructures and its ternary alloys $Mg_xZn_{1-x}O$ and $Cd_xZn_{1-x}O$ have the potential to compete with III–V nitrides for optoelectronic applications [7, 8].

However, in order for ZnO to become commercially applicable, more research needs to be conducted, including on the control of native defect activation and the effects of intrinsic and extrinsic defects on its optical properties. An early study on the evaporation of Zn and ZnO under specific conditions reported in the 1950s [9] showed that the evaporation rate of Zn from ZnO increases slowly at first, then rapidly increases with temperature, reaching its highest rate at ~900 °C (both without and under electron bombardment) and causing intrinsic defects [9]. The formation of intrinsic defects during thermal treatment has been confirmed to have a strong influence on the optical properties of ZnO [10–12]. Taking advantage of these observations, a comprehensive study on the influence of annealing temperature and environment on the surface of ZnO nanorods (ZNs) and on the defect passivation effect of hydrogen on the optical properties of solution-grown ZNs have been reported by our group [13, 14]. The presence of H was confirmed in the near surface region of solution-grown ZNs [13]; the optimum annealing temperature for suppressing H-related centres (H_o) was confirmed to be 450 °C, while annealing at 300 °C significantly increased the ultraviolet emission (UV) at room temperature (*RT*). An asymmetric broadening was observed on the low energy side of the bound exciton photoluminescence in samples annealed below 300 °C and was ascribed to a high concentration of ionized impurities related to hydrogen. This has been

✉ Crispin Munyelele Mbulanga
crispin.mbulanga@nmmu.ac.za

[1] Department of Physics, Nelson Mandela Metropolitan University, 77000, Port Elizabeth 6031, South Africa

Published online: 28 January 2017

attributed primarily to the conversion of hydrogen molecule to substitutional hydrogen on the oxygen site (H_o) as a result of annealing. Furthermore, annealing at high temperature (850 °C) affected the stoichiometry balance of Zn and oxygen as expected [13]. In this paper, we present a photoluminescence (PL) spectroscopy study of the effects of thermal annealing on the deep level emission (DLE) at room temperature in solution-grown zinc oxide nanorods. X-ray photoelectron spectroscopy (XPS) is used as a complementary technique to confirm changes in stoichiometry upon annealing in various environments.

2 Experimental detail

The growth of nanorods by chemical bath deposition (CBD) consisted of two steps: deposition of a ZnO seed layer on a cleaned (001) silicon substrate, followed by deposition of the nanorods on the pre-treated substrate. Full details are provided in Reference [13].

Annealing experiments were conducted in a horizontal quartz tube at different temperatures and in different environments, all at atmospheric pressure. Controlled flows of N_2, O_2, Ar and a mixture of Zn vapour and Ar were used to create the desired annealing environment.

For XPS experiments samples cleaved from one big reference sample were annealed in different environments. Samples were all kept in non-sealed containers (for 12 h) before commencement of XPS investigations. Different samples (from the same reference) were annealed separately at 300, 600, and 850 °C in N_2 and O_2, respectively.

To study the effect of annealing temperature, sections were cleaved from an as-grown sample, one of which was subsequently used as a reference. Note that before annealing, PL spectra were taken from different regions on the reference sample before cleaving to confirm the uniformity of the PL response across each sample. Starting at 300 °C, a single piece of a sample was annealed for 30 min in O_2 ambient. This was followed by a PL measurement, a further 30 min anneal at an increased temperature of 400 °C, and a subsequent PL measurement. This process was repeated, with the annealing temperature ramped up in increments of 100 °C before subsequent PL measurements. The highest annealing temperature was 900 °C. This process will subsequently be referred to as sequential annealing through out the text. The same procedure was repeated for a N_2 ambient. Irrespective of annealing ambient, it was found that 30 min was sufficient to enhance the UV and suppress the deep level emission [14]. As a result, the duration of each annealing step was fixed to 30 min. To investigate the effect of annealing environment, different pieces of a single sample were prepared and annealed at ~900 °C in different ambients and for different times. Note that annealing times given here refer to the times that the samples were kept in the hot zone of the furnace.

A Jeol JSM-7001F field emission scanning electron microscope (SEM) was used to investigate the morphology of the ZNs. The system used for X-ray photoelectron spectroscopy (XPS) analysis is a "PHI 5000 Versaprobe-Scanning ESCA Microprobe". Sputtering was performed with an Ar ion gun at a rate of ~18 nm/min. The excitation X-ray beam of ~100 μm diameter penetrated the sample up to 2 μm in depth, while the detected photoelectrons come from the first 3 to 5 monolayers from the surface. The energy resolution of both instruments is of 0.5 eV and the absolute error for the photoelectron detectors for an angle of incidence of 45° is 2%. The base pressure during XPS experiments was 4×10^{-9} Torr.

Room temperature (RT) PL spectroscopy was used for the analysis of the optical properties of the samples. The emission from the sample was filtered with an appropriate high pass filter (GG385 or KV450, depending on the wavelength range of interest) to filter out the reflected laser light. The detected signal was amplified with a lock-in amplifier connected to a mechanical chopper. Furthermore, based on the band gap of ZnO an IK-series He–Cd laser source (from KIMMON) with a wavelength of 325 nm was used as an excitation source. The output power is 15 mW. A 1 m monochromator (Horiba FHR1000) with a 1800.48 grooves/mm grating (blaze wavelength 400 nm) was used to disperse the PL.

3 Results and discussion

3.1 Effect of annealing temperature and environment on stoichiometry

Figure 1a presents a typical SEM micrograph of as-grown ZnO nanorods used in this study. It is seen that the rods have a hexagonal cross-section. Figure 1b presents the Zn:O ratios $\left(S^X_{Zn,O}\right)$ in sputtered samples as a function of annealing temperature for both N_2 and O_2 atmospheres. These ratios were calculated as follows:

$$S^X_{Zn,O} = \frac{C_{Zn}}{C_O}$$

where C_{Zn} and C_O are, respectively, the concentrations of Zn and O obtained by XPS. The superscript X represents the annealing environment. For quantification purposes the Zn $2p_{3/2}$ and O 1 s XPS peaks were considered. Note that only atomic concentrations measured after sputtering were calculated and considered to minimize contributions from

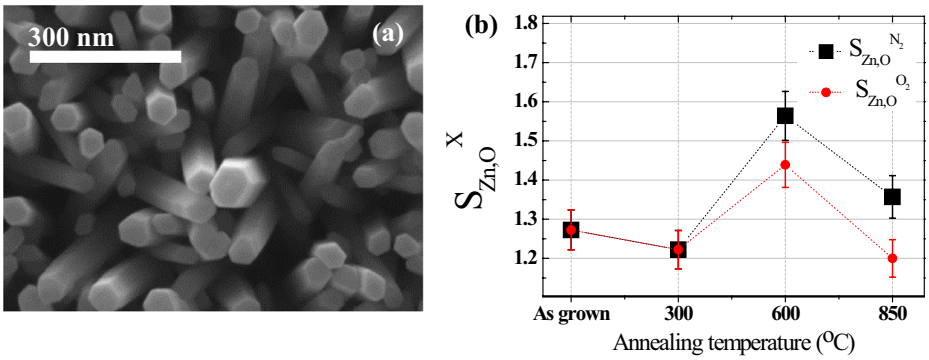

Fig. 1 **a** *Top view* SEM micrograph of as-grown ZnO nanorods at higher magnification. **b** Stoichiometric ratios between Zn and O for samples annealed in N_2 and O_2 as function of annealing temperature. *Dotted lines* are added in (**b**) to guide the eye

surface contamination. The dotted lines are added to the figure to guide the eye. It is also worth noting as well that XPS studies were not performed in situ, i.e. during annealing. Hence, recontamination of the surface from the ambient environment during transferring the annealed samples from the annealing furnace to the XPS facility was inevitable. In an attempt to circumvent this problem, the sample surfaces were Ar-sputtered for XPS measurements and spectra were recorded before and after sputtering.

From Fig. 1b, the following can be concluded: (1) regardless of the annealing ambient and temperature the Zn: O ratios are found to be above 1, indicating that the near surface regions of the rods are rich in Zn. (2) Annealing at 300 °C leaves the stoichiometry unchanged, due to the fact that at this temperature there is no significant thermal energy for the creation of intrinsic defects at concentrations that are detectable by XPS. Furthermore, (3) the largest value measured for $\left(S^{X}_{Zn,O}\right)$ is after annealing at 600 °C.

Theoretical predictions by Kohan et al. [15] related to Zn-rich ZnO agree with the above observations. It was shown that in a Zn-rich ZnO, oxygen vacancies (V_O) forms abundantly at 1000 K (726.85 °C), because of its lower formation energy. The reduced Zn: O ratios (relative to a 600 °C anneal) for the samples annealed at 850 °C is ascribed to the simultaneous loss of O and Zn atoms at this temperature, but at different rates. Furthermore, a clear effect of annealing environment on the ZnO stoichiometry is also observable for high annealing temperatures. It appears that more oxygen is lost from the near surface regions when annealing takes place in a N_2 environment, enhancing the Zn: O ratio compared to samples annealed in oxygen. Since oxygen is a constituent of ZnO it should reduce the evaporation rate of oxygen from the surface, which will result in a comparatively higher loss of oxygen when annealing takes place in nitrogen. This effect is more pronounced at 850 °C.

3.2 Effect of annealing temperature, environment and time on optical properties

Figure 2 shows typical normalized RT PL spectra of ZNs from different cleaved pieces of an as-grown sample. As can be seen, the spectra are very similar, indicating the uniformity of the nanorods. Note that the feature observed at ~759 nm is the second order of the near band emission (NBE). The apparent PL band appearing as a shoulder at around 850 nm (encircled) is induced by the detection limit (cut off) of the detector, while the sharp feature at around 440 nm is from the laser plasma.

Figure 3 shows RT PL spectra of samples sequentially annealed at different temperatures in (a) N_2 and (b) O_2. The intensity of both the UV emission and DLE

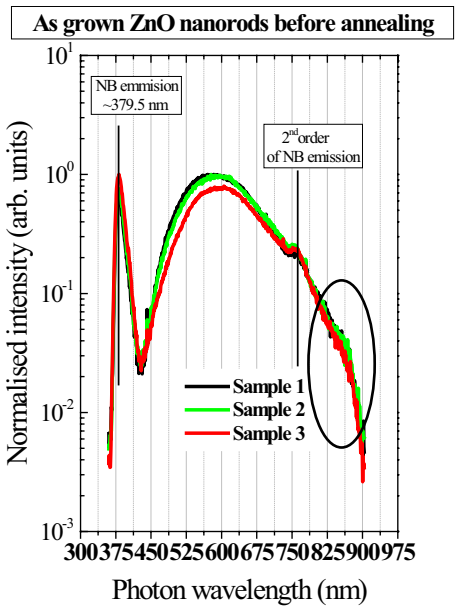

Fig. 2 Typical room temperature PL spectra of ZnO nanorods from three different pieces of an as-grown sample

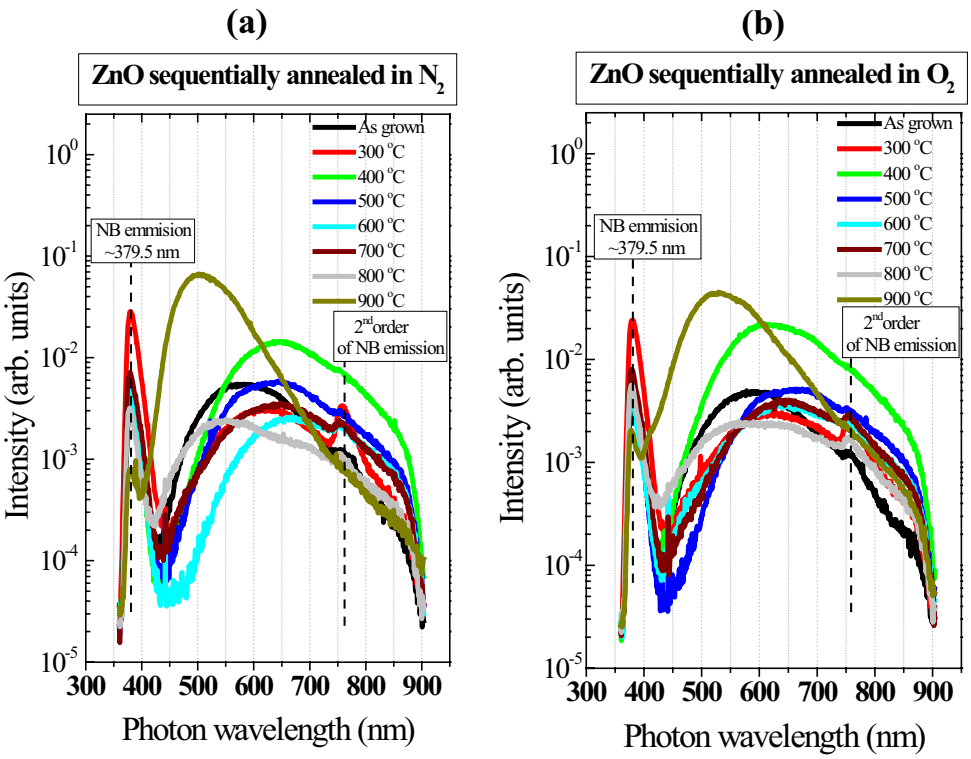

Fig. 3 RT PL of ZnO nanorods annealed sequentially for 30 min in controlled flows of (**a**) N_2 and (**b**) O_2

significantly varies with annealing temperature. In particular, the highest UV emission intensity, irrespective of annealing ambient, is observed from nanorods annealed at 300 °C, while the intensity of the DLE is only slightly decreased after annealing at this temperature. For annealing temperatures greater than 300 °C the intensity of the UV emission decreases. The position of the dominant DLE changes considerably with annealing temperature. Overall, the effect of annealing temperature can be classified into two ranges: 300–600 °C and from 600 to 900 °C. This is emphasized in Fig. 4, where spectra for samples annealed in the lower temperature range are shown in Fig. 4a (N_2 ambient) and (c) (O_2 ambient) and those collected after annealing in the higher temperature range are shown in (b) (N_2) and (d) (O_2). The pink lines are Gaussian fits indicating the positions and widths of the three bands believed to contribute to the DLE following annealing at 900 °C.

From studying the PL as function of annealing temperature, the following remarks can be made: (1) there is an increase in the UV intensity and a concomitant decrease in the DLE intensity after annealing at 300 °C in the green region of the spectrum, irrespective of the annealing environment (see Fig. 4a, c); (2) an overall increase in the DLE intensity is observed after annealing at 400 °C and a simultaneous decrease in the UV intensity occurs (see Fig. 4a, c); (3) a quenching of the DLE is seen above 400 °C (up to 600 °C), irrespective of the ambient, while the UV emission intensity weakly fluctuates (see Fig. 4a, c); (4) based on the spectral changes of the DLE with annealing temperature, the DLE is deduced to be composed of at least two wavelength regions: blue–green (with two emission bands, one at ~500 nm and the other at ~550 nm) and yellow–red (with a band at ~650 nm); and (5) a significant increase in the intensity of the DLE in the blue-green region is evident after annealing at temperatures above 800 °C (see Fig. 4b, d). From remarks (1, 2, 3 and 5) it is understood that the effect of annealing ambient under specified experimental conditions is minimal on the RT optical properties of ZNs. It is important to notice that while annealing at 300 °C significantly enhances the UV emission, the DLE intensity is barely changing. For clarity, the RT PL spectra from nanorods annealed at 300–400 °C, together with those of as-grown nanorods, are re-plotted in Fig. 5. The decrease (300 °C) and increase (400 °C) in the intensity of the dominant DLE are highlighted by the arrows.

The increase in the UV emission intensity and suppression of the defect-related emission following annealing at 300 °C has been observed in solution-grown ZnO nanostructures and is typically attributed to the removal of surface-adsorbed impurities [14]. It was deduced from XPS and ToF-SIMS results [13] that hydrogen is the most abundant surface-adsorbed impurity. It was suggested to introduce band bending near the surface, and therefore influences the PL properties of ZnO [16, 17]. Hence, it is natural to associate the increase in the UV intensity after

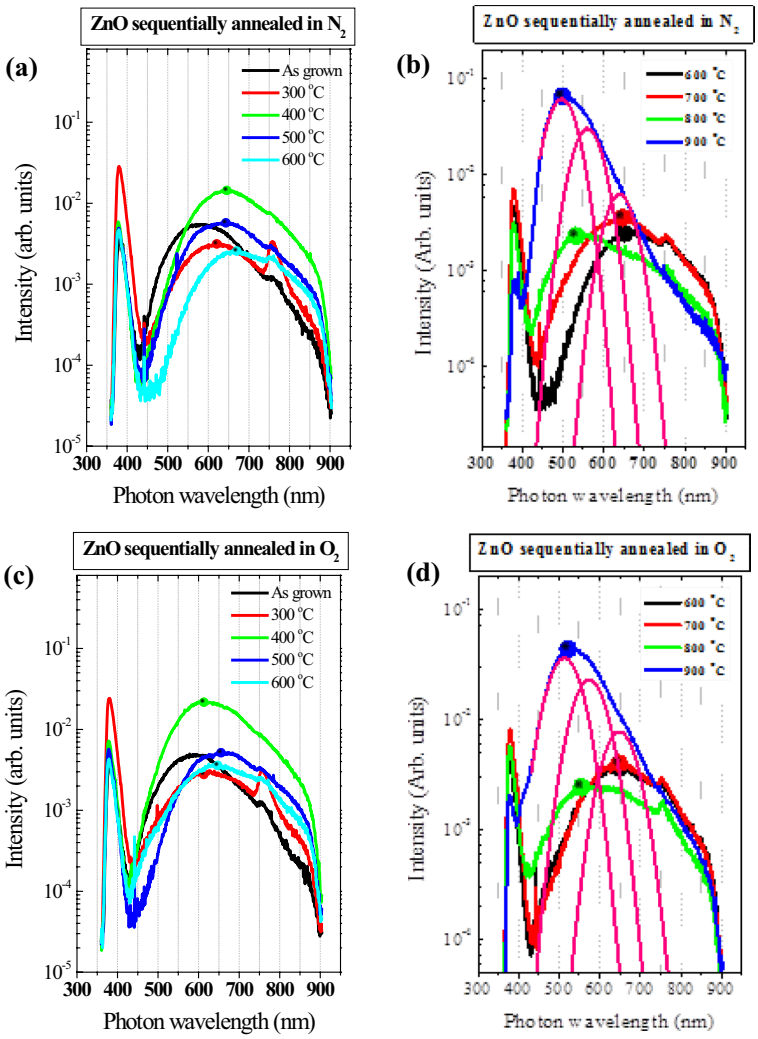

Fig. 4 **a, c** RT PL spectra of samples sequentially annealed between 300 and 600 °C in: (**a**) N_2 and (**c**) O_2 flow. **b, d** RT PL spectra of samples annealed between 600 and 900 °C in (**b**) N_2, and (**d**) O_2 flow. The maximum intensity of the DLE was taken at the spherical dots shown in the figures. *Dotted lines* in (**b**) and (**d**) are Gaussians indicating the positions and widths of the three emission bands deduced to contribute to the visible PL after a 900 °C anneal

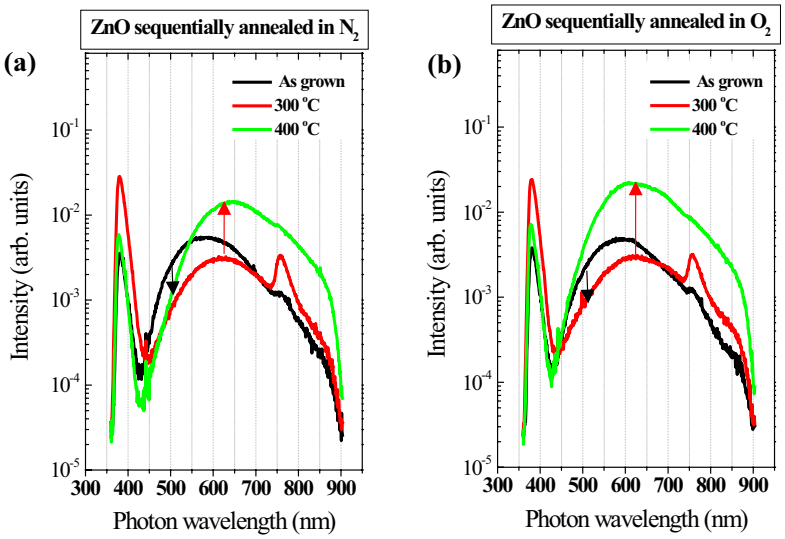

Fig. 5 Comparison of RT PL spectra of ZnO nanorods sequentially annealed in different environments at 300 and 400 °C: **a** in N_2 and **b** in O_2

annealing at 300 °C with the removal or out-diffusion of hydrogen [see remark (1)].

Another reason for the increase in UV emission is the defect passivation effect of hydrogen [14]. For example, Dev et al. [18] observed an enhancement of the near band edge emission and a concomitant quenching of the DLE at room temperature in ZnO nanowires following hydrogen plasma treatment. The authors related the observed enhancement of the NBE emission and decrease in DLE to a large amount of hydrogen incorporated on interstitial sites, providing additional radiative channels for bound exciton recombination and the passivation of deep centres, respectively [18]. Furthermore, in hydrogen plasma-treated ZnO, the formation of H_{Zn} and H_O [19, 20] and the possibility of trapping of H_i in vacancies [21] has been already reported. It has also been reported that hydrogen can form complexes with zinc vacancies ($V_{Zn}H_2$) and with oxygen vacancies (V_OH_2) during hydrogenation [22, 23]. As indicated by XPS and ToF-SIMS results in Ref. [13], hydrogen is part of nanorods deposited by CBD. In addition, we have clearly illustrated the presence of hydrogen in oxygen vacancies (H_O), which gives rise to a low temperature PL line (often labelled as I_4) that is significantly reduced after annealing at 450 °C [24]. The same observation was reported by Herklotz et al. [21]. Furthermore, a closer look at the RT PL spectra of the nanorods annealed at 300 °C (Fig. 5), reveals that the decrease in the DLE intensity after annealing at this temperature [remark (1)] happens only in the region of the spectrum pointed out by black arrows in Fig. 5. Based on this decrease in DLE intensity, it is therefore concluded that annealing at 300 °C does not increase the concentration of new deep centres but rather causes the passivation of existing defects, which is observed in the DLE region mentioned above. This conclusion is in agreement with the XPS results in Fig. 1a, which indicates no change in stoichiometry upon annealing at low temperatures (300 °C). Given the relatively low annealing temperature (300 °C), and based on the abundance of H-related defects in as-grown nanorods, the enhancement of the UV intensity and the slight quenching of the DLE irrespective of the annealing ambient are also ascribed to the passivation of defects by hydrogen.

As the annealing temperature increases further from 300 to 400 °C, defects previously passivated by hydrogen (H_O and/or H_{Zn}) will be activated, resulting in an enhancement of the DLE and a decrease in the UV emission intensity [remark (2)]. As indicated above, the out-diffusion of H has been confirmed by the disappearance of the I_4 line from the low temperature PL spectrum after annealing at ~450 °C [24]. Additionally, the removal of hydrogen-related defects in hydrogenated ZnO after annealing at 450 °C was also deduced from RT PL in Ref [22].

Another contributing factor to the increase in DLE after annealing at 400 °C is the dissociation of existing complexes, such as V_OZn_i [25] into V_O and Zn_i. Theoretical investigations by Kim et al. [25] have shown that in Zn-rich ZnO, Zn_i and V_O can interact and form stable V_OZn_i complexes (at RT) that contribute to the n-type conductivity of undoped ZnO. They investigated the interaction of a zinc interstitial (Zn_i) with an oxygen vacancy (V_O) to understand the origin of native *n*-type ZnO, using density functional theory with the hybrid functional. The authors found that the V_OZn_i complex has a lower formation energy than the sum of the individual point defect formation energies, and that it creates a shallow donor with +1 charge state [25]. Given the fact that as-grown nanorods are Zn-rich (see Fig. 1b), the existence of these complexes in as-grown material is quite likely. Hence, the overall increase in the DLE intensity upon increasing the annealing temperature from 300 to 400 °C, is suggested to result from a combination of the out-diffusion of hydrogen in vacancies (V_O or/and V_{Zn}) and the dissociation of complexes such as V_OZn_i.

The quenching of the DLE following annealing at a temperatures between 400 and 600 °C [remark (3)] is associated with the activation of "hidden" interstitial H_2 [23] or H_2 molecules trapped in the oxygen vacancy [26] that convert into atomic hydrogen during annealing. By combining local mode and free carrier infrared (IR) absorption measurements, Shi et al. [26] studied the effect of annealing on as-received hydrothermally grown ZnO substrate. They reported an IR line at 3326.3 cm^{-1} (at 4 K) which was activated only after annealing near 400 °C. The intensity of this line increased with annealing temperature between 400 and 500 °C and then vanished upon annealing at 600° [26]. The same line could be produced after hydrogenation at 725 °C and subsequent quenching to RT. The donor (hydrogen) [27] was unstable, annealing out at 150 °C, but could be reactivated (presumably from the dissociation of "hidden" molecular hydrogen) by annealing near ~450 °C and above [26]. It was suggested therefore, that there exists a reservoir of hydrogen molecules which thermally dissociate between ~400 and ~600 °C into H-related defects; and a kind of cyclic hydrogen passivation effect takes place causing the observed quenching of the DLE.

Finally, the increase in DLE intensity upon high temperature annealing [remark (5)] is associated with the degradation of the sample (i.e. the creation of new point defects). D'art [9] has studied the evaporation rate of ^{64}Zn from ZnO as a function of annealing temperature (between ~150 and ~900 °C), both with and without electron bombardment, using mass spectometry. In his experiments the author detected two ion peaks, one for an ion with mass 64 amu (atomic mass units) corresponding to Zn, and one for an ion with mass 80 amu corresponding to ZnO. Because ^{64}Zn is the most

abundant zinc isotope in nature and to avoid any possibility of varying background contamination, the evaporation of ZnO was followed by measuring the ^{64}Zn ions produced. It was found that without electron bombardment Zn atoms start to evaporate at ~700 °C [9]. An exponential increase in evaporation rate was reported for temperatures up to ~900 °C [9]. This indicates that annealing near this temperature (~900 °C) results in the formation of new Zn-related defects due to ZnO evaporation. Based on these findings, the overall observed increase in the intensity in the DLE following annealing between ~700 and ~900 °C, irrespective of annealing ambient, is associated with the effect of the degradation of the ZnO. Attempts to explain the origin of the observed bands as mentioned in remark (4), are reported below.

3.3 Effect of annealing environment on the optical properties of nanorods

Unfortunately under the annealing conditions discussed so far, RT PL spectroscopy of the nanorods does not reveal any significant effect of the ambient, unlike the results obtained by XPS. The failure to observe the effect of the environment on the DLE emission at RT under these annealing conditions does not necessary imply that the ambient has no effect. Studies on the surface stoichiometry showed that the ambient does indeed affect the creation of native defects in the rods.

To observe optically the effect of annealing environment on the DLE, pieces of material were sequentially annealed for different periods of time at a temperature where point defects are known to be readily generated (i.e. above 800 °C).

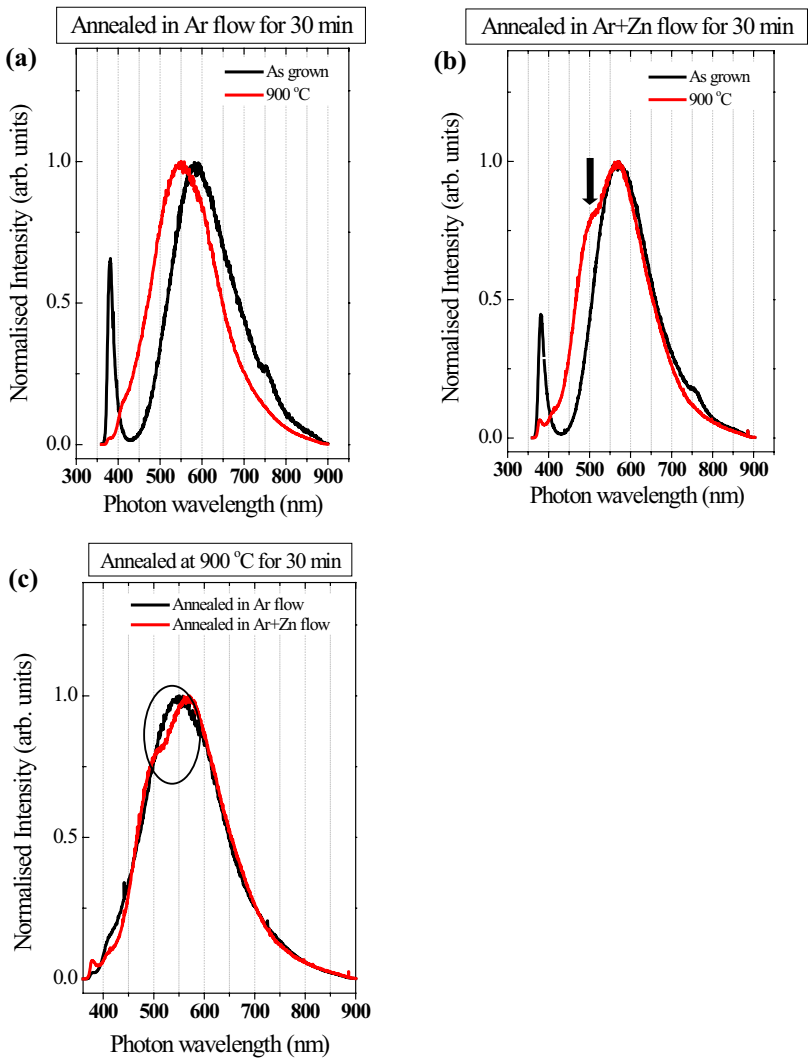

Fig. 6 **a** RT PL spectra for samples annealed in Ar. **b** RT PL spectra for samples annealed in Ar and Zn vapour. **c** RT PL spectra of annealed samples extracted from (**a**) and (**b**) for comparison purposes

Figure 6a, b compare normalized RT PL spectra of as-grown nanorods to those of samples annealed for 30 min at 900 °C in (a) a controlled flow of Ar and (b) a controlled flow of Ar plus Zn vapour from a pure Zn plate upstream from the sample. Figure 6c compares the normalized RT PL spectra of the annealed nanorod samples from Fig. 6a, b. It is worth also noting that the melting point of Zn is 419.53 °C and the boiling point ~907 °C [28]. From Fig. 6a, it is seen that annealing in an Ar flow only caused a significant activation of defects, predominantly radiating in the blue–green part of the spectrum. From Fig. 6b it is seen that the addition of Zn vapour during annealing caused the same effect, but with a slight difference: the activation of the defects emitting in the blue-green part of the spectrum was reduced. This is more clearly depicted in Fig. 6c (see encircled region). It is thus concluded that the presence of Zn during annealing at 900 °C primarily affects the green deep emission band (~500 nm), which is suggested to involve V_{Zn}—related defects. The same assignment of the green luminescence activated at 900 °C was made recently by Wang et al. [29]. Using positron annihilation spectroscopy, the authors showed that the introduction of the green luminescence (~500 nm) in undoped ZnO grown by pulsed laser deposition correlated with the formation of V_{Zn} at 900 °C.

To confirm the above assignment, another annealing experiment was conducted at 900 °C, in which the aim was to passivate V_{Zn}—related defects. Figure 7 presents RT PL spectra of nanorods sequentially annealed in different environments and at different temperatures. First, the rods were annealed in an Ar flow for 30 min at 800 °C, to activate intrinsic defects. As a result, the DLE was enhanced (see red spectrum in Fig. 7). The sample was subsequently annealed for another minute in the same Ar flow, but with Zn vapour also present in the flowing gas stream. After this 1 min annealing step, the DLE was quenched and partially resolved, while the UV emission was enhanced (see the green spectrum in Fig. 7a). To confirm the authenticity of these bands, a filter with 450 nm cut-off wavelength (KV450) was placed in front of the monochromator. The quenching of the green band observed previously (see Fig. 6b or c) is again evident in these figures. The enhancement in UV emission intensity is presumably due to the annihilation of V_{Zn} by Zn atoms. Therefore, it is strongly suggested that the observed green DLE band at ~500 nm results from V_{Zn}—related defects. This being so, the DLE quenching observed upon annealing at 300 °C of ZNs [see remark (1)] is understood to have been caused by V_{Zn}—defect passivation by hydrogen.

The origins of the bands at longer wavelengths [~550 nm (or 575 nm)], ~650 nm and 750 nm are unknown at present.

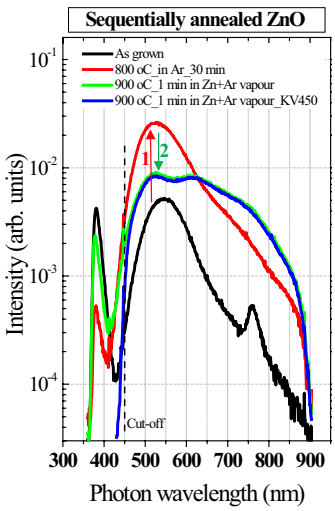

Fig. 7 RT PL spectra of ZnO nanorods annealed sequentially in Ar at 800 °C and then at 900 °C in Ar and Zn vapour. The numbered arrows indicate subsequent spectral developments caused by (*1*) annealing in Ar, and (*2*) annealing in Ar and Zn vapour

4 Conclusion

Zinc oxide nanorods (ZNs) grown by a two-step chemical bath deposition method on Si substrate were characterized. As-grown ZNs were thermally treated and studied for a better understanding of the optical properties at room temperature, with the emphasis on the visible luminescence. To this end, thermal treatments of as-grown ZNs were conducted under different conditions for a study of the defect-related photoluminescence.

XPS showed that the near surface regions of solution-grown ZNs are rich in Zn. Annealing further changes the Zn/O stoichiometry ratios. Within the detection limit of XPS, it was confirmed that O and Zn-rich ambients of annealing affect the activation of intrinsic defects.

Thermal treatment at high temperatures (400–800 °C) removed H-related defects. This caused significant changes in the room temperature luminescence properties of ZNs nanorods, quenching and enhancing deep level emission, especially when samples were annealed sequentially from 300 to ~700 °C. Specifically, the passivation of vacancy-related defects by H was demonstrated following thermal treatment in this temperature range.

The evolution of the green luminescence (~500 nm) following annealing above ~800 °C suggested that this band involves Zn vacancy defects. Hence, the quenching observed in the DLE upon annealing at 300 °C is ascribed to the passivation of Zn vacancies.

Acknowledgements This work is based upon research supported by the South Africa Research Chairs Initiative of the Department of Science and Technology and the National Research Foundation (NRF),

South Africa. The financial support from Nelson Mandela Metropolitan University (NMMU) is also gratefully acknowledged.

References

1. A. Umar, M.M. Rahman, S.H. Kim, Y.B. Hahn, "ZnO nanonails: synthesis and their application as glucose biosensor". J. Nanosci. Nanotechnol. **8**, 3216 (2008)
2. S. Al-Hill, M. Willander, "Membrane potential measurements across a human fat cell using ZnO nanorods". Nanotechnol. **20**, 175103 (2009)
3. J.C. Johnson, H.J. Choi, K.P. Knutsen, R.D. Schaller, P. Yang, R.J. Saykally, "Single gallium nitride nanowire lasers". Nat. Mater. **1**, 106 (2002)
4. A.B. Greytak, C.J. Barrelet, Y. Li, C.M. Lieber, "Semiconductor nanowire laser and nanowire waveguide electro-optic modulators". Appl. Phys. Lett. **87**, 151103 (2005)
5. M. Law, D.J. Sirbuly, J.C. Johnson, J. Goldberger, R.J. Saykally, P. Yang, "Nanoribbon waveguides for subwavelength photonics integration". Sci. **305**, 1269 (2004)
6. H. Zhang, J.B. Wu, C.X. Zhai, N. Du, X.Y. Ma, D.R. Yang, "From ZnO nanorods to 3D hollow microhemispheres: solvothermal synthesis, photoluminescence and gas sensor properties". Nanotechnol. **18**, 455604 (2007)
7. K. Talla, J.K. Dangbegnon, M.C. Wagener, J. Weber, J.R. Botha, "Effect of growth parameters on MgxZn(1-x)O films grown by metalorganic chemical vapour deposition". J. Cryst. Growth **315**, 297 (2011)
8. L. Pavesi, "Silicon-based light sources for silicon integrated circuits". Adv. Opt. Technol. **2008**, 1 (2008)
9. F.E. Dart, "Evaporation of zinc and zinc oxide under electron bombardment". Phys. Rev. **78**, 761 (1950)
10. T.M. Børseth, B.G. Svensson, A.Y. Kuznetsov, P. Klason, Q.X. Zhao, M. Willander, "Identification of oxygen and zinc vacancy optical signals in ZnO". Appl. Phys. Lett. **89**, 262112 (2006)
11. K.E. Knutsen, A. Galeckas, A. Zubiaga, F. Tuomisto, G.C. Farlow, B.G. Svensson, A.Y. Kuznetsov, "Zinc vacancy and oxygen interstitial in ZnO revealed by sequential annealing and electron irradiation". Phys. Rev. B **86**, 121203 (2012)
12. Z. Fang, Y. Wang, D. Xu, Y. Tan, X. Liu, "Blue luminescent center in ZnO films deposited on silicon substrates". Optical Mat. **26**, 239 (2004)
13. C.M. Mbulanga, Z.N. Urgessa, S.R. Tankio Djiokap, J.R. Botha, M.M. Duvenhage, H.C. Swart, "Surface characterization of ZnO nanorods grown by chemical deposition". Phys. B **480**, 42 (2015)
14. Z.N. Urgessa, C.M. Mbulanga, S.R. Tankio Djiokap, J.R. Botha, M.M. Duvenhage, H.C. Swart, "The defect passivation effect of hydrogen on the optical properties of solution-grown ZnO nanorods". Phys. B **480**, 48 (2015)
15. A.F. Kohan, G. Ceder, D. Morgan, "First principles study of native point defects in ZnO". Phys. Rev. B **61**, 15019 (2000)
16. Z.M. Liao, H.Z. Zhang, Y.B. Zhou, J. Xua, J.M. Zhang, D.P. Yu, "Surface effects on photoluminescence of single ZnO nanowires". Phy. Lett. A **372**, 4505 (2008)
17. I. Shalish, H. Temkin, V. Narayanamurti, "Size-dependent surface luminescence in ZnO nanowires". Phys. Rev. B **69**, 245401 (2004)
18. A. Dev, R. Niepelt, J.P. Richters, C. Ronning, T. Voss, "Stable enhancement of near-band-edge emission of ZnO nanowires by hydrogen incorporation". Nanotechnology **21**, 065709 (2010)
19. E.V. Lavrov, F. Herklotz, J. Weber, "Identification of two hydrogen donors in ZnO". Phys. Rev. B **79**, 165210 (2009)
20. J.J. Dong, X.W. Zhang, J.B. You, P.F. Cai, Z.G. Yin, Q. An, X.B. Ma, P. Jin, Z.G. Wang, P.K. Chu, "Effects of hydrogen plasma treatment on the electrical and optical properties of ZnO films: identification of hydrogen donors in ZnO". Appl. Mater. Interface **2**, 1780 (2010)
21. F. Herklotz, E.V. Lavrov, J. Weber, "Photoluminescence study of hydrogen donors in ZnO". Phys. B **404**, 4349 (2009)
22. Y.M. Strzhemechny, J. Nemergut, P.E. Smith, J. Bae, D.C. Look, "Remote hydrogen plasma processing of ZnO single crystal surfaces". J. Appl. Phys. **94**, 4256 (2003)
23. M.-H. Du, K. Biswas, "Anionic and hidden hydrogen in ZnO", Phys. Rev. Lett., **106**, 115502 (2011)
24. Z.N. Urgessa, J.R. Botha, M.O. Eriksson, C.M. Mbulanga, S.R. Dobson, S.R. Tankio Djiokap, K.F. Karlsson, V. Khranovskyy, R. Yakinova, P.-O. Holtz, "Low temperature near band edge recombination dynamics in ZnO nanorods". J. Appl. Phys. **116**, 123506 (2014)
25. D.-H. Kim, G.-W. Lee, Y.-C. Kim, "Interaction of zinc interstitial with oxygen vacancy in zinc oxide, An origin of n-type doping". Solid State Commun. **152**, 1711 (2012)
26. G.A. Shi, M. Saboktakin, M. Stavola, S.J. Pearton, "Hidden hydrogen in as-grown ZnO". Appl. Phys. Lett. **85**, 5601 (2004)
27. M.D. Mc Cluskey, S.J. Jokela, K.K. Zhuravlev, P.J. Simpson, K.G. Lynn, "Infrared spectroscopy of hydrogen in ZnO". Appl. Phys. Lett. **81**, 3807 (2002)
28. International zinc association, Zinc. http://www.zinc.org/basics/zinc_properties. Accessed 25 May 2015
29. Z. Wang, S.C. Su, M. Younas, F.C.C. Ling, W. Anwand, A. Wagner, "The Zn-vacancy related green luminescence and donor–acceptor pair emission in ZnO grown by pulsed laser deposition". R. Soc. Chem. (RSC Adv.) **5**, 12530 (2015)